

Thermal conductivity and electrical resistivity of gadolinium as functions of pressure and temperature

P. Jacobsson and B. Sundqvist

Department of Physics, University of Umeå, S-901 87 Umeå, Sweden

(Received 20 April 1989)

The electrical resistivity ρ and the thermal diffusivity a of gadolinium have been measured as functions of T in the range 45–400 K. The thermal conductivity λ has been calculated from a and experimental data for the specific-heat capacity, c_p . λ can be analyzed in terms of simple models for the lattice and electronic components above the Curie temperature $T_C \approx 291.4$ K. Below T_C an additional term, identified as a magnon (spin-wave) thermal conductivity λ_m , is found. ρ and λ have also been studied as functions of T and P in the range 150–400 K and 0–2.5 GPa. The Lorenz function $L = \rho\lambda/T$ increases by about 20%/GPa under pressure due to a very strong pressure dependence of the lattice thermal conductivity. The pressure coefficients of ρ and λ are -5.1×10^{-2} and 0.22 GPa^{-1} , respectively, at 300 K (above T_C), and 0 and 0.16 GPa^{-1} at 200 K (below T_C). T_C and the spin-reorganization temperature $T_r \approx 219$ K both decrease under pressure, at the rates -14.0 and -22.0 K/GPa , respectively. Although the magnitude of λ_m cannot be accurately calculated from the zero-pressure data for λ , the temperature dependence of $d\lambda/dP$ allows us to distinguish between several models and assign a value of $\lambda_m \approx 1.5 \text{ W m}^{-1} \text{ K}^{-1}$, or 16.0% of λ , at 200 K.

I. INTRODUCTION

Gadolinium is a rare-earth metal with incomplete filling of the $4f$ electronic shell which leads to spontaneous magnetic moments localized on the ions, causing ferromagnetism. Even though the conduction electrons are not themselves responsible for the magnetism, there is a connection between magnetic order and transport properties, since the valence electrons are strongly scattered by these moments.^{1,2}

Although the electrical resistivity ρ of Gd is well known, the available data^{3–13} for the thermal conductivity λ differ very much between different sources: the magnitude of λ differs by more than a factor of 2 at room temperature even between recent investigations. The differences in slope $d\lambda/dT$ are much larger than this, and exotic conduction mechanisms have been invoked to explain the temperature dependence.^{3,4} In an attempt to clarify this situation, we report here measurements of the thermal- and electrical-transport properties of Gd as functions of both temperature T and pressure P . We have previously studied both λ and ρ for other ferromagnetic metals such as Ni and Fe (Refs. 14 and 15) under pressure, and we were especially interested in studying the behavior of $\lambda(P)$ and $\rho(P)$ near T_C , which for Gd is conveniently situated near room temperature. Also, we were interested in comparing the behavior of $\rho(P, T)$ for ordered and disordered Au-Cu alloys¹⁶ with that of magnetically ordered and disordered Gd.

We have been able to obtain new, accurate data for both λ and ρ as functions of T and P . The new data for λ are lower than most published results, but in excellent agreement with those from a recent investigation at higher temperatures.⁸ The data can also be analyzed using simple models, except that we observe a residual

magnon-thermal-conductivity term below T_C . To our knowledge, such a term has not previously been identified in any metal above 100 K.

In Sec. II of this paper we describe some experimental details. Section III then contains our experimental results, giving zero-pressure and high-pressure data separately. These results are then discussed in some detail in Sec. IV. Finally, we repeat again the most important findings in Sec. V.

II. EXPERIMENTAL DETAILS

Since most of the details concerning the experimental methods and the equipment used are published elsewhere,^{16,17} we shall only give a brief description here.

The gadolinium specimen was obtained in the form of wire, 1 mm in diameter, from Goodfellows Metals, England. The stated purity was 99.9% and to avoid contamination and oxidation all handling was done under silicone oil or argon. The specimen was annealed in a vacuum for 10 h at 750 K (Ref. 18) before the first measurement, and again after the thermocouple wires were torn off during a preliminary high-pressure test.

We have not measured λ directly but instead the thermal diffusivity, a , using two dynamic periodic methods. a is defined as $a = \lambda/dc_p$, where d is the density and c_p the specific-heat capacity. At atmospheric pressure a was measured using the original Ångström method,¹⁹ and at high pressure using a modified two-frequency method.¹⁷ In both methods, a sinusoidal temperature wave is created in one end of a rod. The temperature variations are measured at two points, using the specimen itself as one leg of a differential thermocouple. a can be calculated from the phase shift and the attenuation and then, knowing d and c_p , λ can be calculated. In

the original Ångström method, radial heat losses by radiation are automatically taken into account. In the modified method two frequencies are used, which makes it possible also to eliminate heat loss by conduction.¹⁷ The scatter in the final diffusivity data was less than 0.5% rms using Ångström's original method, and about 3% using the modified method. The dominating source of systematic errors is the uncertainty in the distance between the thermocouples, which could introduce an error of up to 2% in a . The equipment used is described in detail in Ref. 16.

R was calculated from the voltage drop over the sample and over a 10 m Ω standard resistor connected in series, respectively, at a dc current of ≈ 0.1 A. To avoid thermoelectric effects current reversal was always used, and the temperature gradient in the specimen was minimized by varying T slowly (1 K/min). The resolution in the resistance measurements was 10 $\mu\Omega$, equivalent to an uncertainty of 0.02 $\mu\Omega$ cm in the resistivity. Above 40 K the uncertainty in ρ was 1% due to the uncertainty in the geometrical dimensions.

The low-pressure experiments were carried out at pressures below 10^{-1} torr, and in an argon atmosphere above room temperature to reduce the possibility of oxidation of the specimen. Temperatures down to 30 K were obtained using a closed-cycle He compressor system (Leybold-Heraeus RW5+RG1040), and above room temperature a simple vacuum oven was used.

The high-pressure measurements were carried out in two piston and cylinder devices, 70 and 45 mm in diameter, respectively.¹⁶ As shown previously²⁰ it is important in this experiment to use a pressure-transmitting medium which has a high viscosity and still is hydrostatic. Also, to avoid oxidation we need an inert medium which does not dissolve water. The medium used in most of the present experiments was a silicone oil (Dow Corning DC 200, viscosity grade 100 mm²/s), which unfortunately solidifies at about 1 GPa at room temperature.²¹ Nonhydrostatic pressure-transmitting media cause strain in the specimen when changing the pressure, and to prevent this we always raised T to above 400 K to melt the medium before changing the pressure at $P > 0.5$ GPa. We have checked the hydrostatic properties of the oil by comparing the data for ρ obtained in oil with those found using a 50/50 mixture of n -pentane and isopentane, hydrostatic to > 5 GPa,²² and found excellent agreement up to about 1.5 GPa. Also, in our isobaric experiment (see below) we see no anomalies in either ρ or a that can be attributed to solidification of the medium.

III. EXPERIMENTAL RESULTS

A. Results at atmospheric pressure

1. Electrical resistivity

The electrical resistivity of Gd has been studied previously at normal pressure.^{3-13,23,24} Except for differences in the residual resistivity and determination of the spin reorganization point at about 220 K all studies show almost the same T dependence. We have calculated ρ from

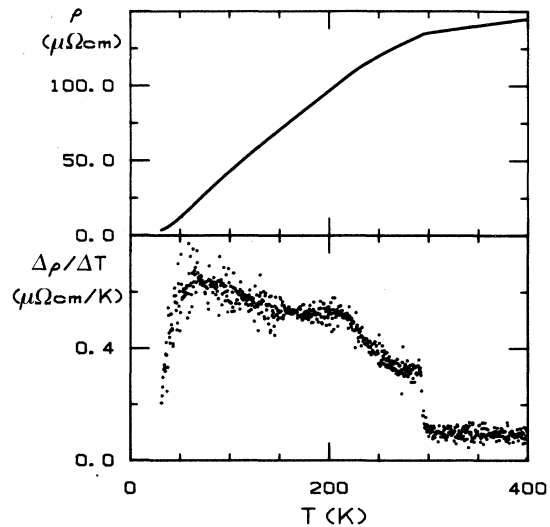


FIG. 1. Upper part: ρ vs T . Lower part: $\Delta\rho/\Delta T$ between successive data points vs T .

the measured data for R and from the geometrical dimensions with correction for thermal expansion.²⁵ Figure 1, upper part, shows ρ versus T between 30 and 400 K at P less than 10^{-1} torr. Interpolated data are also shown in Table I. Taking the differences in residual resistivity into account, our data agree with all of Refs. 3-13, 23, and 24 to within the combined experimental errors at 300 K. For example, Binkele⁸ gives $\rho = 134.9$ $\mu\Omega$ cm at 300 K while Powell and Jolliffe⁶ find $\rho = 134$ $\mu\Omega$ cm at 291 K. When comparing single-crystal and polycrystal electrical resistivities for hcp metals the proper relationship is

TABLE I. Experimental data for ρ , a , λ , and L at selected temperatures.

T (K)	ρ ($\mu\Omega$ cm)	$10^6 a$ (m ² s ⁻¹)	λ (W m ⁻¹ K ⁻¹)	$10^8 L$ (W Ω K ⁻²)
30	3.7			
45	9.2	15.2	13.3	2.75
60	17.9	11.3	12.8	3.87
80	30.6	9.4	12.5	4.81
100	42.8	8.2	11.9	5.13
150	70.5	6.4	10.6	5.02
200	96.6	5.2	9.4	4.56
250	119.7	4.0	8.4	4.04
291.4	133.5	2.6	7.9 ^a	3.62 ^a
300	135.3	4.4	8.0	3.61
350	140.2	5.1	8.1	3.29
400	144.8	5.4	8.6	3.10
600	157 ^b		10.9 ^b	2.9 ^b
800	171 ^b		12.7 ^b	2.7 ^b
1000	183 ^b		14.4 ^b	2.6 ^b
1200	195 ^c	9.5 ^c	15.5 ^c	2.48 ^c

^a λ and L data at T_C are uncertain, see text.

^bReference 8 (the data are taken from presented figures).

^cReference 12.

$\rho_{\text{poly}} = (\rho_c + 2\rho_a)/3$, where the subscripts a and c denote the basal plane direction and the principal axis direction, respectively. From the single-crystal data of Nellis and Legvold¹⁰ we find $\rho_{\text{poly}} = 133.6 \mu\Omega \text{ cm}$, in good agreement with our data.

In the lower part of Fig. 1 we show $\Delta\rho/\Delta T$, as calculated between every two consecutive data points. From these data we have determined the Curie point $T_C = (291.4 \pm 0.5) \text{ K}$ and the spin reorganization temperature $T_r = (219 \pm 2) \text{ K}$. Our value for T_C shows good agreement with data from the literature for polycrystalline Gd. Bloch and Pavlovic²⁶ have collected T_C data from seven papers, finding a mean value of $(291.8 \pm 0.6) \text{ K}$. This value is lower than reported values for single-crystal specimens: Hargraves *et al.*²⁷ report $T_C = 293.51 \text{ K}$ and Nellis and Legvold¹⁰ report $T_C = 293 \text{ K}$. The differences between the polycrystalline and the single-crystal data have already been noted by Bartholin and Bloch.²⁸ They found that the difference in T_C was in agreement with the variations in the exchange energy between the magnetic ions. It is also known²⁹ that T_C in Gd decreases with increasing impurity content. However, since this decrease is not very rapid, the difference between T_C data cannot be explained solely by variations in the purity between the specimens. Data from the literature^{3,24,30} for T_r differ between 224 and 235 K, and torque measurements of the temperature dependence of the easy direction of magnetization^{31,32} show discrepancies of the same amount. It is argued³¹ that these discrepancies arise from different intrinsic strains and impurities.

2. Thermal diffusivity, thermal conductivity, and Lorenz function

In Fig. 2 we show our measured data for the thermal diffusivity between 40 and 400 K at P less than 10^{-1} torr. Interpolated data of a are also presented in Table I. It is obvious that a is a smooth function of T except at T_C , where the rapid change of c_p gives rise to a pronounced dip in a . The scatter in the data is less than 0.5% rms, which must be added to the (temperature-independent) systematic error discussed above. At temperature near T_C we have an additional uncertainty in a due to the temperature difference of about 5 K between the measurement points on the specimen. The measured a is always an average value over this temperature range. Near T_r only a very small change in da/dT is seen; however, in one single temperature run we observed a narrow dip in a at T_r , similar in depth to that at T_C . This dip is probably connected with the cusp observed³⁰ in c_p at T_r , but since it was not repeatable it will not be discussed further. We know of no previous measurements of a in this temperature range with which to compare our data.

The thermal conductivity λ was calculated from our data for a , interpolated to every 5 K, together with data for thermal expansion,²⁵ density (7.895 g cm^{-3} at 298 K), and specific-heat capacity. The c_p data between 40 and 230 K were taken from Griffel *et al.*³³ and between 270 and 400 K from Fransson;³⁴ over the range 230–270 K the data were smoothly interpolated between these two

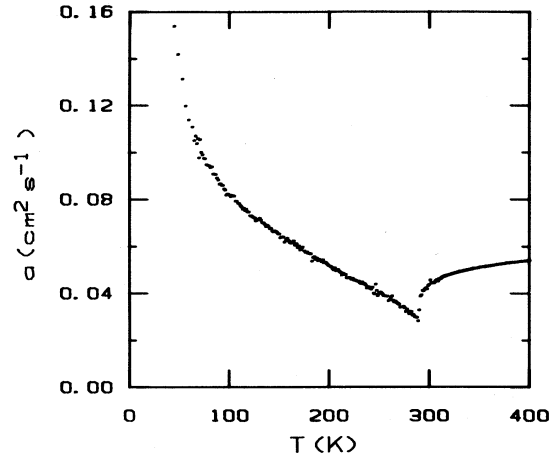


FIG. 2. Thermal diffusivity as a function of T .

sets. The measurements of Ref. 34 were made with a Perkin-Elmer DSC-2 Differential Scanning Calorimeter on a piece taken from our specimen. The maximum error given is $< 1.5\%$ except at $T \approx T_C$ where a large temperature gradient in the specimen, arising from the low value of a , increases the error to 2.5%. Between 200 and 355 K, where the two sets of data overlap, the data of Griffel *et al.* are 0.8–2% higher than those of Fransson.

Our calculated data for λ are presented in Table I and in Fig. 3. To a very good approximation, λ is linear in T both above and below T_C , with a small change of slope near T_r . At T_C , our data show a small peak. This is an artifact arising from the smearing of the diffusivity data near T_C , and would disappear if similarly integrated data for c_p had been used in the calculation. The true λ shows a sharp minimum at a temperature identical to the value of T_C obtained from the resistivity data, in contrast to several previous determinations.^{3–5,9} The possible error

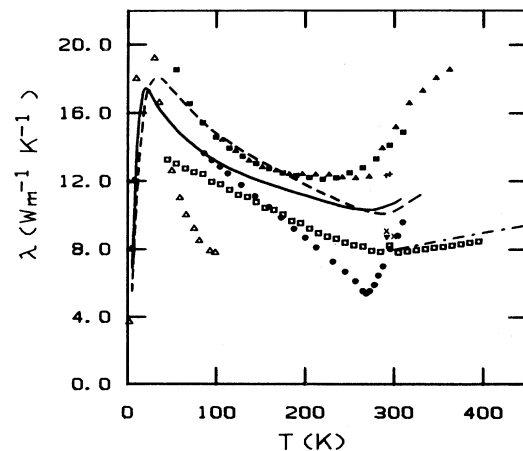


FIG. 3. Thermal conductivity as a function of T . \square , this work; \blacktriangle , Ref. 3; $+$, Ref. 4; \blacksquare , Ref. 5; upper \times , Ref. 6; lower \times , Ref. 7; $-\cdot-\cdot-$, Ref. 8; \bullet , Ref. 9; solid curve and dashed line, Ref. 10 (a and c axis); \blacktriangledown , Ref. 11; \triangle , Ref. 13.

in λ is obtained by adding the respective errors in a , c_p , and d , and consists of a temperature-independent systematic error less than 2.5% due to the error in d and the thermocouple distance, and a random error less than 1.5% from the data for c_p and the scatter in the data for a .

There are several previous papers³⁻¹³ reporting data for the thermal conductivity of Gd, and we show data from many of these in Fig. 3. Only one paper deals with single crystals.¹⁰ The agreement between the different sets of data is, even for polycrystalline specimens, strikingly poor. At low temperatures the disagreement could be caused by varying purities and different physical states for the different specimens. The purities reported for the specimens studied are 99.9% in Refs. 8-13 and 99.99% in Ref. 3, while no numerical information is given in Refs. 4-7. We see little correlation between the reported purities and the thermal conductivities for the data presented in Fig. 3. However, the majority of these studies have been carried out using steady-state methods, in which the inherent experimental error due to radiation heat loss increases rapidly with increasing T . Although this error can, in principle, be corrected,^{11,35} it is actually very difficult to carry out this correction. It has already been noted¹¹ that the very high values sometimes reported for Gd could be due to this mechanism.

Our data agree with the recent Kohlrausch-method data of Binkele⁸ to well within the combined experimental error, and reasonably well also with the data of Powell and Jolliffe,⁶ who used two different comparator methods, and the steady-state data of Cranch¹¹ and Legvold and Spedding.⁷ The single-crystal data of Nellis and Legvold,¹⁰ obtained with a longitudinal-steady-state method, show a similar temperature dependence but are about 20% higher than our data. Since grain-boundary scattering should be important only at very low temperatures, we would have expected the agreement with our data to become better at high temperatures.

The high-temperature data of Binkele⁸ are in very good agreement with the data of Novikov *et al.*,¹² who also calculated λ from measured data for a . We suggest that

for polycrystalline Gd a reliable set of data for the thermal-transport properties can be obtained by combining our data with those of Binkele and those of Novikov *et al.*, as presented in Table I.

Using our data for λ and ρ we have calculated the Lorenz function $L = \lambda\rho/T$. As can be seen in Fig. 4, L is a smooth function of T . In contrast to previous studies^{3-5,9} we see only a small change of slope at T_C , and the mutual agreement between our data and those of Binkele⁸ and Novikov *et al.*¹² is excellent. The combined data indicate a continuous approach towards the standard Sommerfeld value $L_0 = 2.45 \times 10^{-8} \text{ W } \Omega \text{ m/K}^2$ at very high temperatures.

B. High-pressure results

1. Electrical resistivity

We have measured R as a function of T under isobaric conditions and as a function of P under isothermal conditions. Using thermal expansion data²⁵ and compressibility data³⁶ we have calculated ρ from R and the geometrical dimensions. Figure 5 shows ρ versus T from 200 to 360 K in four isobaric runs. We made nine such isobaric runs, and in all of these ρ was linear in T above T_C . For two separate experiments with four isobaric runs in each we have calculated $d(\ln\rho)/dP$ to be -5.4×10^{-2} and $-4.7 \times 10^{-2} \text{ GPa}^{-1}$, respectively, at 295 K. Below T_C $d(\ln\rho)/dP$ increases continuously with decreasing T , reaching zero at about 210 K. In Table II we present $d(\ln\rho)/dP$ as a function of T .

At pressures above approximately 2 GPa Gd undergoes a transition from the hcp structure to a phase with the Sm-type structure.³⁷⁻³⁹ This phase is claimed to be paramagnetic, possibly with a helimagnetic structure at low temperature.³⁷ In Fig. 6 we show data from two isothermal pressure runs at 295 K, the first using silicone oil and the second using a 50/50 mixture of *n*- and isopentane as pressure-transmitting media. In both runs, the transition can be seen to occur at about 2.0 GPa under

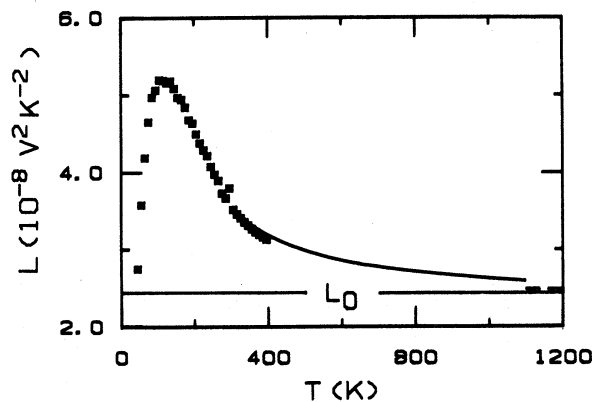


FIG. 4. Temperature dependence of L . Squares, this work; solid curve, Ref. 8; dashed line, Ref. 12.

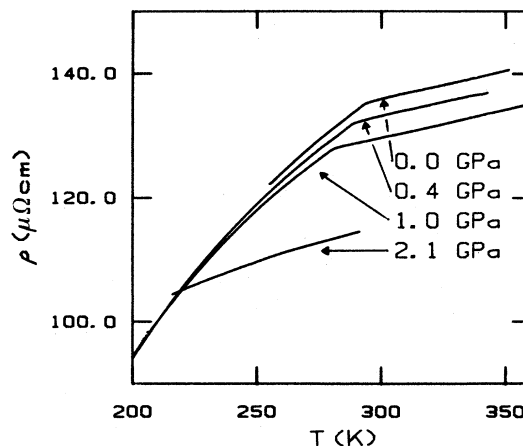


FIG. 5. ρ vs T at the pressures indicated.

TABLE II. Pressure dependence of ρ , a , c_p , and λ at selected temperatures.

T (K)	$\rho^{-1}d\rho/dP$ (GPa $^{-1}$)	$a^{-1}da/dP$ (GPa $^{-1}$)	$c_p^{-1}dc_p/dP$ (GPa $^{-1}$)	$\lambda^{-1}d\lambda/dP$ (GPa $^{-1}$)
150	0.013 ^a	0.16	0.04	0.20
200	-0.004 ^a	0.09	0.07	0.16
250	-0.022	0.05	0.13	0.18
275	-0.028	-0.05	0.25	0.20
300	-0.051	0.29	-0.08	0.22
350	-0.051	0.26	-0.03	0.24
400	-0.050 ^a	0.25	-0.02	0.23

^aValues obtained by extrapolating the experimental data.

increasing pressure, where there is a sudden decrease in R by 5.0% in the first run and 4.8% in the second. In the first run, solidification of the oil causes strain in the specimen and thus a departure from linearity in ρ above 1.5 GPa. In the second run we cooled the cell to 200 K at 2.1 GPa, as shown in Fig. 5 and discussed below, before releasing pressure at 245 K. Both at 295 and 245 K the high-pressure phase was metastable to about 0.5 GPa on decreasing P . In the hcp phase R decreases linearly with increasing pressure, and we calculate $d(\ln\rho)/dP = -5.0 \times 10^{-2}$ and -5.2×10^{-2} GPa $^{-1}$ for the two runs at 295 K. Including the data from the isobaric runs we obtain a mean value of $d(\ln\rho)/dP = -5.1 \times 10^{-2}$ GPa $^{-1}$ at 295 K.

The pressure dependence of ρ below 2.5 GPa at room temperature has been studied many times before.⁴⁰⁻⁴² From Bridgman's⁴⁰ measured $d(\ln R)/dP$ we find $d(\ln\rho)/dP = -5.2 \times 10^{-2}$ GPa $^{-1}$, and from the figures of Fujii *et al.*⁴¹ and Stromberg and Stephens⁴² we calculate $d(\ln\rho)/dP = -5.8 \times 10^{-2}$ and -3.6×10^{-2} GPa $^{-1}$, respectively. Austin and Mishra⁴³ report

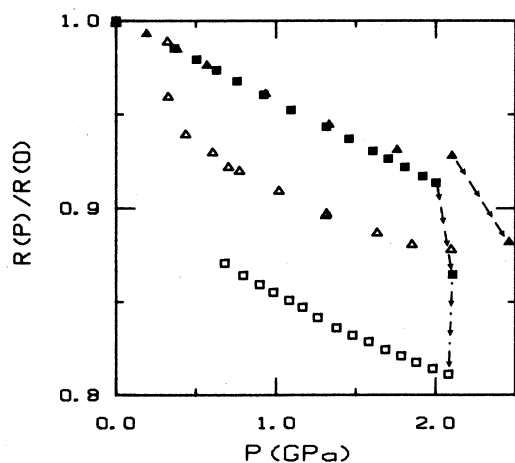


FIG. 6. $R(P)/R(P=0)$ vs P . \blacktriangle , first run, increasing P at 295 K; \triangle , first run, decreasing P at 295 K; \blacksquare , second run, increasing P at 295 K; \square , second run, decreasing P at 245 K. Data points before and after the hcp-to-Sm-type transition are connected with dashed lines. The dot-dashed line represents the temperature decrease from 295 to 245 K shown in Fig. 5.

$d(\ln\rho_m)/dP = -8.4 \times 10^{-2}$ GPa $^{-1}$ in the c -axis direction, where ρ_m is the magnetic disorder component of ρ (to be discussed further below). The hcp-to-Sm-type structure transition was previously observed by Bridgman but not, surprisingly, by Stromberg and Stephens.

As discussed above and shown in Fig. 5 we made one isobaric run at 2.1 GPa to see whether we could observe any transition to a magnetically ordered phase. We observe a small change in $d\rho/dT$ at about 260 K, close to the expected value for T_C as linearly extrapolated from atmospheric pressure. We believe that this anomaly simply indicates that the specimen contains a small amount of untransformed hcp phase, as also observed by McWhan and Stevens.³⁸

From the isobaric data for ρ we have also determined the pressure dependence of the critical temperature T_C and T_r . We find $dT_C/dP = (-14.0 \pm 0.5)$ K GPa $^{-1}$ and $dT_r/dP = (-22.0 \pm 2.0)$ K GPa $^{-1}$. We know of no data in the literature for dT_r/dP , but for dT_C/dP we have calculated a mean value of 11 determinations^{26,36,44,45} as $dT_C/dP = -14.6$ K GPa $^{-1}$.

2. Thermal diffusivity and thermal conductivity

The thermal-transport properties of Gd have never been studied under pressure before. In Fig. 7 the temperature dependence of a is shown at three different pressures. Each symbol represents the mean value of 5-8 separately measured data points. The general behavior of a versus T is the same at all P , and we note that the pressure coefficient is much smaller below T_C than above, in agreement with the results for ρ . This is also obvious from Table II, where we present our data for $d(\ln a)/dP$ as a function of T . In one of the isothermal pressure experiments shown in Fig. 6 we also measured a at 317 K to 2.45 GPa, through the hcp \rightarrow Sm transition. The pressure coefficient below the transition was in excellent agreement with the results already shown. In the high-pressure phase, a was found to be 15% higher than in the hcp phase, but with practically the same pressure

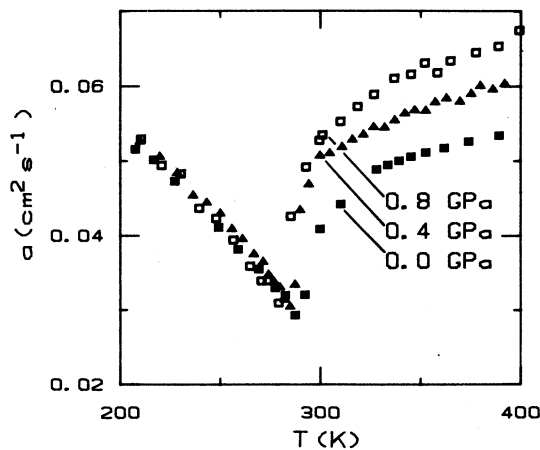


FIG. 7. Thermal diffusivity vs T at the pressures indicated.

coefficient in the range of metastability. Although the high value of a is of some interest, we cannot deduce the value of λ in the high-pressure phase due to the lack of data for c_p , and we shall not discuss this result further in this paper.

In order to calculate the pressure dependence of λ we must know the pressure dependences of c_p and d . The latter is found from the compressibility, but no data are available for the pressure dependence of c_p , although c_p for Gd has in fact been studied under pressure by Jura and Stark.⁴⁴ Unfortunately they used their method solely to determine dT_C/dP .

We have previously,^{16,20} for simpler metals, calculated dc_p/dP from the volume thermal expansion coefficient α_v , through the thermodynamic identity⁴⁶

$$(\partial c_p / \partial P)_T = -(T/d)[\alpha_v^2 + (\partial \alpha_v / \partial T)_P]. \quad (1)$$

For simple metals dc_p/dP is small, and any errors arising from uncertainties in α_v or $\partial \alpha_v / \partial T$ are of little importance for the final result for $d\lambda/dP$. In the present case, however, both α_v and c_p contain significant magnetic components which could be expected to show an appreciable pressure dependence, and we are not sure that Eq. (1) gives sufficiently accurate results for our needs. We have instead tried to separate the lattice, electronic, and magnetic components of both $c_p(T)$ and $\alpha_v(T)$. The magnetic part of the heat capacity, c_{pm} , is associated with the magnetic order which diminishes rapidly above T_C . We have assumed that c_{pm} is zero at 400 K and that the electronic part $c_{pe} = \gamma_e T$ at all T . The constant γ_e is found to be $4.05 \times 10^{-5} \text{ J g}^{-1} \text{ K}^{-2}$ from low-temperature data for c_p .⁴⁷ To the remaining part c_{pl} at 400 K we fit a Debye function with $\Theta_D = 163.4 \text{ K}$,⁴⁷ and c_{pm} is obtained by subtracting c_{pl} and γT from c_p . The lattice part of α_v is estimated by simply extrapolating the thermal expansion data²⁵ from the paramagnetic region down to 150 K.

The pressure dependence of c_{pl} is found by applying Eq. (1) to the lattice component of α_v , and we find $d(\text{inc}_{pl})/dP = -2 \times 10^{-2} \text{ GPa}^{-1}$, practically independent of T between 150 and 400 K. For c_{pe} we use⁴⁸ $c_{pe} = (\pi^2/3)k^2 T N(E_F)$, where k is Boltzmann's constant and $N(E_F)$ is the electronic density of states at the Fermi energy E_F . We then find $d(\text{inc}_{pe})/dP = d(\ln N(E_F))/dP = -7.5 \times 10^{-2} \text{ GPa}^{-1}$ as given by Darby and Richardson.⁴⁹ Since c_{pe} is a small part of c_p , however, even this large pressure coefficient adds little to the total $d(\text{inc}_p)/dP$. The pressure dependence of c_{pm} is difficult to estimate, and we have tried two ways of doing this: In the first model, we assumed that both the total magnetic energy $E_m = \int c_{pm} dT$ and the function $c_{pm} = c_{pm}(T/T_C)$ are independent of P . We then found c_{pm} at 1 GPa by simply multiplying $c_{pm}(T/T_C)$ by $T_C(0 \text{ GPa})/T_C$ (1 GPa). However, this model did not agree well without experimental data for a near T_C , from which we can measure the height of the peak in c_p as the inverse of the dip in a . We find that the height increases by 26% GPa^{-1} , while the model just described gives 5.1%. We have therefore in our final calculation used only the assumption that the function $c_{pm}(T/T_C)$ is independent of P ,

and calculated the magnitude of this function at elevated pressures from the measured height of the peak at T_C . The final data for $d(\text{inc}_p)/dP$ are given as a function of T in Table II. It is obvious that both the magnitude and the temperature dependence of this quantity are dominated by the pressure dependence of c_{pm} .

The final calculated data for $d(\ln \lambda)/dP$ are presented in Table II. The pressure dependence of λ is very large, both compared with the results for the metals previously studied^{15,16,20} and compared with $d(\ln \rho)/dP$; in fact, $d(\ln L)/dP \approx 0.2 \text{ GPa}^{-1}$ at all T . The temperature dependence of $d(\ln \lambda)/dP$ is, however, qualitatively similar to that of $d(\ln \rho)/dP$, with a step change at T_C .

IV. DISCUSSION

A. Electrical resistivity under pressure

Since all theories for the transport properties of metals are derived assuming constant volume conditions, the correct procedure in the analysis would be to start by converting all data to constant volume, since data for the thermal expansion, the compressibility, and the pressure dependence of both λ and ρ are available. We have not carried out this procedure, mainly because the difference between constant volume conditions and constant pressure conditions should be small in the present case: most of our data are obtained between 150 and 400 K, in which range the net thermal expansion is small.²⁵

For the electrical resistivity ρ we shall use the standard assumption⁵⁰ that

$$\rho = \rho_0 + \rho_{ep} + \rho_m, \quad (2)$$

where ρ_0 is the residual resistivity and ρ_{ep} and ρ_m are due to scattering by phonons and magnetic spins, respectively. ρ_m is assumed to be constant above T_C (Ref. 50) where the spin disorder is complete, although this assumption has been questioned.⁵¹ The slope $d\rho/dT$ above T_C is thus assumed to be due entirely to phonon scattering. ρ_0 cannot be found directly from the measured data since the lower-temperature limit here is 30 K. We have estimated an upper limit to ρ_0 by first removing ρ_{ep} from our data by fitting a Bloch-Wilson equation, with $\Theta = 163.4 \text{ K}$, to the high- T ($> T_C$) data. This should give a marginally better estimate of ρ_{ep} at 30 K than a simple linear function $\rho = AT$. From $\rho - \rho_{ep}$ we estimate $\rho_0 \leq 2.9 \mu\Omega \text{ cm}$. $\rho_m(T)$ is then found as $\rho - \rho_{ep} - \rho_0$ and above T_C $\rho_m = 104.1 \mu\Omega \text{ cm}$.

The high-pressure results obtained in the isobaric runs were analyzed in the same way, but with $\rho_{ep} = AT$ since $T > \Theta$, and assuming $\rho_0(P) = \rho_0(0)$. Two experiments were made, each comprising four isobaric runs at different pressures, but with different pressure media. We have chosen to use the results obtained using pentane rather than silicone oil, partly because this is a "better" pressure medium, but mainly because data were taken over a wider range in T . However, similar results were obtained in both experiments. Somewhat surprisingly, we find that ρ_{ep} increases with increasing pressure, with $d(\ln \rho_{ep})/dP = 1.8 \times 10^{-2} \text{ GPa}^{-1}$. The pressure

coefficient of ρ_m is strongly temperature dependent, as shown in Fig. 8. This is due to the large, negative dT_C/dP . If we assume $\rho_m = Bf(T/T_C)$, where B depends on V but not on T , and differentiate with respect to P we obtain

$$\frac{1}{\rho_m} \frac{\partial \rho_m}{\partial P} = \partial(\ln B)/\partial P - \frac{T}{T_C} \frac{\partial T_C}{\partial P} \partial(\ln \rho_m)/\partial T. \quad (3)$$

From data for ρ_m at $P=0$ we have calculated the second term β (shown in Fig. 8) and subtracted it from the measured $\partial(\ln \rho_m)/\partial P$. The resulting $d(\ln B)/dP$, also shown in Fig. 8, is independent of T , except for a dip near T_C which arises because we use an average $d\rho_m/dP$ between 0 and 1 GPa, thus smearing the sharp behavior of $d(\ln \rho_m)/dT$. Our assumption that ρ_m is the same function f of normalized temperature T/T_C at all pressures, and that the "true" $d(\ln \rho_m)/dP = d(\ln B)/dP = -6.4 \times 10^{-2} \text{ GPa}^{-1}$, independent of T/T_C , is thus verified. As a comparison, Fujii *et al.*⁴¹ find $d(\ln \rho_m)/dP = -8.3 \times 10^{-2} \text{ GPa}^{-1}$, and Austin and Mishra⁴³ $-8.4 \times 10^{-2} \text{ GPa}^{-1}$ (along the c axis).

The pressure dependence of ρ_m has been discussed previously, and it is usually assumed⁵² that

$$\rho_m = K_1 m^* J^2 / V E_F, \quad (4)$$

where m^* is the effective mass and J is the indirect exchange constant. Combining Eq. (4) with the expression $T_C = K_2 J^2 / V^2 E_F$ in a free-electron model, it is possible to find the pressure or volume dependence of m^* and J

from the pressure dependence of ρ_m and T_C . (In these expressions, the constants K_1 and K_2 are assumed independent of P .) From our data we find $d(\ln m^*)/dP = 1.0 \times 10^{-2} \text{ GPa}^{-1}$, very close to the value calculated in a free-electron model, and $d(\ln J)/dP = -4.6 \times 10^{-2} \text{ GPa}^{-1}$, both intermediate between previous data.⁵²

The positive sign for $d\rho_{ep}/dP$ is unusual for a pure metal. At high temperature, ρ_{ep} can be written⁴⁸

$$\rho_{ep} = 8\pi^2 k T \Lambda_{tr} / (h \omega_p^2), \quad (5)$$

where $\omega_p^2 = 8\pi e^2 \langle v_F^2 \rangle N(E_F) / 3V$ is the Drude plasma frequency, v_F is the Fermi velocity, and the transport electron-phonon interaction factor Λ_{tr} is defined as

$$\Lambda_{tr} = \int [\alpha_{tr}(\omega)]^2 F(\omega) d\omega / \omega. \quad (6)$$

Here $[\alpha_{tr}(\omega)]^2$ is the transport electron-phonon coupling and $F(\omega)$ is the density of phonon states. It is easily shown that⁵³

$$\begin{aligned} (d^2 \rho_{ep} / dT dP) / (d\rho_{ep} / dT) \\ = d(\ln \Lambda_{tr}) / dP - 2d(\ln \omega_p) / dP. \end{aligned} \quad (7)$$

In our case ρ_{ep} is a linear function $C(1+DT)(1+EP)$ of T and P , and $(d^2 \rho_{ep} / dT dP) / (d\rho_{ep} / dT) \equiv d(\ln \rho_{ep}) / dP$ at $P=0$. If we use again the free-electron model, where⁴⁸ $\omega_p^2 = 4\pi n e^2 / m^*$, we can use our previous result for $d(\ln m^*)/dP$ to find $d(\ln \Lambda_{tr})/dP = -0.2 \times 10^{-2} \text{ GPa}^{-1}$, or practically zero. The increase in ρ_{ep} with P thus seems to be due to the increase in electron effective mass under pressure. We note, however, that the free-electron model is probably not a good approximation for Gd.⁵⁴

B. Thermal conductivity and Lorenz function at $P=0$

In magnetic metals heat can be transported by electrons, phonons, and magnons:

$$\lambda = \lambda_e + \lambda_p + \lambda_m. \quad (8)$$

Above T_C it is believed⁵⁰ that the mean free path for magnons is too short, due to the almost complete spin disorder, for the magnon contribution to be important. The thermal conductivity is then dominated by the first two terms in Eq. (8).

We begin by discussing the electronic part of λ , which can be related to the electrical resistivity already discussed. We write for the thermal resistivity W , in analogy with Eq. (2),

$$\lambda_e^{-1} = W_e = W_{e0} + W_{ep} + W_{em}, \quad (9)$$

where the subscript interpretation is obvious. The largest component in ρ above 60 K is ρ_m , which⁵⁵ may be treated as due to an elastic scattering mechanism. We can then write $W_{em} = \rho_m / T L_0$, probably to a very good approximation. Similarly, we write $W_{e0} = \rho_0 / T L_0$. In simple metals ρ_{ep} and W_{ep} are related by the approximate relation⁴⁸

$$W_{ep} = \rho_{ep} / L_e T, \quad (10a)$$

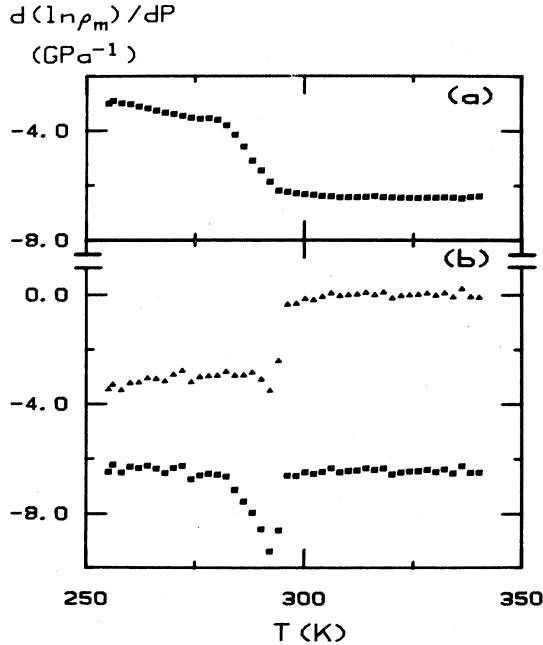


FIG. 8. Pressure dependences of ρ_m as a function of T . (a) Experimental data for $d(\ln \rho_m)/dP$. (b) Triangles, β from Eq. (3); squares, true pressure dependence of ρ_m .

where L_e is the electronic Lorenz function

$$L_e = \frac{2(T/\Theta)^2 J_5(\Theta/T)}{J_3(\Theta/T) + J_5(\Theta/T)/2\pi^2} L_0, \quad (10b)$$

and J_i are Debye integrals of order i . At high T ($T \gg \Theta$) $L_e \rightarrow L_0$. For a metal-like Gd, with a complicated band structure, we would expect L_e to deviate from Eq. (10b); in transition metals such deviations, due to inelastic scattering processes, are common.⁵⁶ However, since $\rho_{ep} \ll \rho_m$, and thus $W_{ep} \ll W_{em}$, such deviations should not be a serious source of error. We have calculated λ_e from our data for ρ under these assumptions, and the result is shown as a dashed line in Fig. 9(a). We note that λ_e is only 45–75% of the total λ , leaving a large residual term to be accounted for. We shall devote most of the remaining part of this section to a discussion of this residual term, treating the temperature ranges above and below T_C separately.

Above T_C , λ_m should be negligible and the difference between λ and λ_e should be entirely due to λ_p . Fitting a polynomial to $(\lambda - \lambda_e)^{-1}$, the best fit is obtained for $(\lambda - \lambda_e)^{-1} = -0.013 + 1.45 \times 10^{-3} T$, with a standard deviation of 2.6%, in excellent agreement with the expected temperature dependence for a lattice thermal conductivity limited by phonon-phonon scattering. The negative in-

tercept is equivalent to only 1% of the total λ at T_C .

We check the assumptions made by extrapolating ρ , λ_e , and λ_p , as obtained above, to high temperatures. λ_e is calculated assuming that ρ_m and ρ_0 are constant, and that $\rho_{ep} = 8.98 \times 10^{-8} T \Omega \text{ cm}$. We add λ_p , as found from the fit above, and find $L = 2.56 \times 10^{-8} \text{ W } \Omega \text{ m/K}^2$ at 1100 K, intermediate between the values 2.58×10^{-8} and 2.49×10^{-8} obtained by Binkele⁸ and by Novikov *et al.*,¹² respectively, at this temperature. We take this to be strong evidence that (a) the extra term in λ above T_C is due to a lattice thermal conductivity limited by phonon-phonon scattering, and (b) L_e does not deviate significantly from L_0 at high temperature. We see no need to invoke other heat transport mechanisms, such as bipolar heat conduction,^{3,4} in this temperature range.

We now turn to the temperature range below T_C . If we extrapolate λ_p , as obtained above, to lower temperatures, we find that $\lambda_e + \lambda_p$ is up to 8% lower than the experimental data for λ between 115 K and T_C . This is also illustrated in Fig. 9(a), where we show both the difference $\lambda - \lambda_e$ (solid squares) and the extrapolated high-temperature behavior of λ_p (solid curve). Whenever the latter is smaller than $\lambda_e - \lambda_p$ we also show the difference (triangles). We have come to the conclusion that this difference must be due to an additional heat current, for the following reasons.

(1) Although the total possible experimental error in λ is 4%, any temperature-dependent errors are smaller than 1.5%, and the discrepancy is thus very much larger than any experimental errors.

(2) The high-temperature data indicate that L_e cannot exceed L_0 by more than 1–2%, and even using such a value for L_e on the total ρ does not significantly change the size of the discrepancy. To explain the anomaly from any error in our calculated λ_e it is necessary to assume that the Lorenz function $L_m = \rho_m / W_{em} T$ is 15–20% higher below T_C than above, which seems unreasonable.

(3) Regarding λ_p , it is conceivable that there could be some extra scattering mechanism operating only above T_C , but we fail to find such a mechanism. On the contrary, we believe that λ_p^{-1} could instead increase below T_C , where phonon-magnon scattering might become important. The term due to scattering by electrons should also be almost independent of T at $T > \Theta$ (see below).

Since we thus cannot find any other explanation, we must identify this additional term in λ as a magnon heat conductivity term λ_m . Such a component has previously been observed⁵⁷ in ferro- and antiferromagnetic metals and insulators. However, in metallic materials magnon thermal conductivity has previously only been identified at very low temperatures.

In order to obtain a better estimate of the magnitude of λ_m we have tried to improve the analysis of the lattice thermal conductivity λ_p . Above, we have only taken phonon-phonon scattering into account, but at low temperatures phonon-electron and phonon-magnon scattering might also be important. We shall neglect the latter term, since this effect is known⁵⁸ to be small in Gd, but in metals λ_p is usually⁵⁹ limited by electron scattering at $T \ll \Theta$. We write

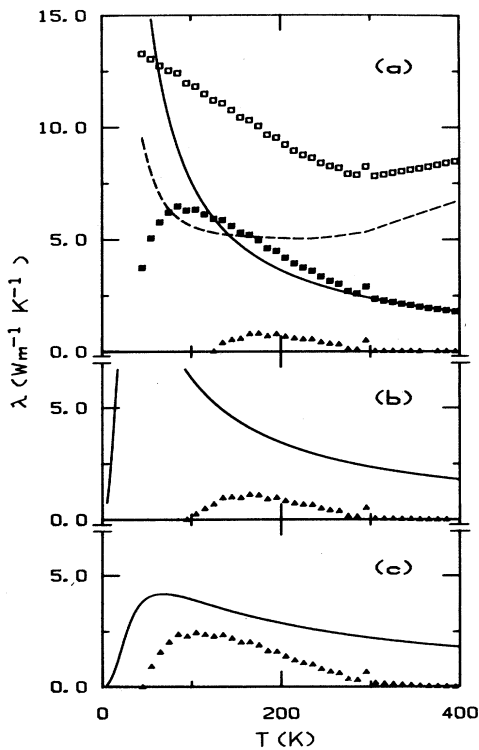


FIG. 9. (a) Thermal conductivity vs T . \square , our experimental data for λ ; dashed line, λ_e calculated from ρ ; solid curve, $\lambda_p \propto T^{-1}$; \blacksquare , $\lambda - \lambda_e$; \blacktriangle , λ_m . (b) solid curve, λ_p (model I); \blacktriangle , λ_m . (c) solid curve, λ_p (model II); \blacktriangle , λ_m .

$$\lambda_p^{-1} \equiv W_p = W_{p-p} + W_{p-e}, \quad (11)$$

where W_p is the lattice thermal resistivity and subscripts $p-p$ and $p-e$ designate scattering by phonons and electrons, respectively. In a Debye model, W_{p-e} can be written⁵⁹

$$W_{p-e} = \frac{2.36[aN(E_F)h\Lambda/k](\Theta/T)^2}{J_3(\Theta/T)}, \quad (12)$$

which, in the limit $T \rightarrow 0$, reduces to $W_{pe} \propto T^{-2}$. Here a is the cube root of the atomic volume, $\Lambda = \int [\alpha(\omega)]^2 F(\omega) d\omega/\omega$, and Λ differs from Λ_{tr} in that the latter weights the interaction proportional to $1 - \cos\Phi$, where Φ is the scattering angle.

As a first approximation (called model I in the following) we estimate $W_{p-e}(T \rightarrow 0)$ from the experimental data of Ratnalingham and Sousa,⁶⁰ who find a quadratic term $\lambda \approx 0.026T^2 \text{ W m}^{-1} \text{ K}^{-1}$. W_{p-e} is then $W_{p-e} = 280/T^2 J_3(\Theta/T)$, which at $T > T_C$ reduces to $W_{p-e} \approx 0.021 \text{ W}^{-1} \text{ K m}$. Using this value, a new fit to the data for $\lambda - \lambda_e$ above 360 K gives a value $W_{p-p} = 1.36 \times 10^{-3} \text{ T W}^{-1} \text{ K m}$, differing by less than 6% from the previous value. The new data for λ_p and λ_m obtained in this way are shown in Fig. 9(b). The agreement between the model and the experimental data for λ_p is still fairly poor below 100 K, which could be due to impurity or magnon scattering.

In order to find a better estimate we have increased the term W_{p-e} until the agreement between the theoretical function $\lambda_p(T)$ and the experimental points extends to the lower limit of our temperature range. The result of this model, here called model II, is shown in Fig. 9(c), where the terms λ_p and λ_m are almost equal in magnitude. Since we will take no account of magnon or impurity scattering this analysis will actually give an upper limit on λ_m , except at low temperatures where the model gives an unrealistically abrupt drop to zero. W_{p-p} is now $1.08 \times 10^{-3} \text{ T W}^{-1} \text{ K m}$, while the low- T limit of $\lambda_p \approx 0.004T^2 \text{ W m}^{-1} \text{ K}^{-1}$, well below the experimental value.⁶⁰ However, to this we should add the low- T limit of λ_m , which should have a T^2 dependence.⁵⁷ The experimental high-temperature ratio $W_{e-p}/W_{p-e} = 0.28$ can be compared with the semiclassical value⁶¹ $W_{e-p}/W_{p-e} = 3/\pi^2 n_a^2$. Good agreement is found for $n_a = 1$ electron per atom, while for Gd $n_a = 3$. However, using Eq. (5) with $L = L_0$, together with the high-temperature limit for W_{p-e} given by Butler and Williams,⁵⁹ it is easily shown that n_a^{-2} in a Debye model should be replaced by $\Lambda_{tr}/\Lambda N(E_F)a\omega_p^2$, which is not unlikely to differ significantly from the free-electron value.

In theory, we could also calculate the components of λ_p . W_{p-p} can be found from any of the various Leibfried-Schlömann-type formulas,⁶²

$$W_{p-p} = K_4 \gamma^2 T / a \Theta^3, \quad (13)$$

where γ is the Grüneisen parameter. However, data from literature⁶³ for γ vary from 0.55 to 1.62, and although a value can be chosen to make the theoretical value for W_{p-p} equal to the experimental value, this is of

little physical interest. W_{p-e} can be calculated from the low-temperature limit⁵⁹ of Eq. (12); inserting $N(E_F) = 1.82 \text{ eV/atom}$ (Ref. 54) and $\Theta = 163.4 \text{ K}$, and taking $\Lambda = 0.3$ as suggested by Tsang *et al.*,⁴⁷ we find $\lambda_p = W_{p-e}^{-1} = 0.013T^2 \text{ W m}^{-1} \text{ K}^{-1}$, intermediate between the values found above.

The two models studied are both fairly realistic, although we have excluded scattering of phonons by both impurities and magnons, and we have still no way of choosing between them. We therefore postpone any discussion of λ_m until after we have discussed the pressure dependence of λ .

C. Thermal conductivity at high pressure

The most striking feature of our high-pressure data (Table II) is the very large pressure coefficient of L at all temperatures; $d(\ln L)/dP \approx 0.2 \text{ GPa}^{-1}$, independent of T . This could be due to some error in the experiment or in the subsequent calculation of λ , but the experimental data are internally consistent, and our method has been tested many times before. A prime suspect might be the large values found for dc_p/dP , but in the range above T_C where $d\lambda/dP$ is largest the data for dc_p/dP are very similar to those for other metals. We thus believe that the high values of $d\lambda/dP$ are real, and we proceed to find an explanation.

We would not expect the electronic Lorenz function to depend much on volume above Θ ,¹⁵ and we can thus calculate λ_e from our measured data for ρ , as before. It is then obvious from the large difference between $d(\ln \rho)/dP$ and $d(\ln \lambda)/dP$ that the very strong pressure dependence of λ must be due mainly to λ_p . In particular, since W_{p-e} should have a pressure dependence similar to that of W_{e-p} (see above), most of this strong pressure dependence must come from W_{p-p} . Using again the simple Leibfried-Schlömann expression⁶² the volume dependence of W_{p-p} is easily shown to be

$$d(\ln W_{p-p})/d(\ln V) \approx 3\gamma + 2d(\ln \gamma)/d(\ln V) - \frac{1}{3}, \quad (14a)$$

where

$$\gamma = \alpha_v / d\kappa_v = -d(\ln \Theta)/d(\ln V) \quad (14b)$$

and κ is the compressibility. The volume dependence of γ is usually not known, and the left-hand side of (7) is often estimated¹⁵ as $4\gamma < d(\ln W_{p-p})/d(\ln V) < 7\gamma$. In the present case, however, we have tried to calculate $d(\ln \gamma)/d(\ln V)$ from data from literature for κ as a function of T and P .^{36,64} We find a surprisingly large $d(\ln \gamma)/d(\ln V) \approx 7.9$, which together with $\gamma = 0.55$ (Ref. 63) gives a theoretical value $d(\ln W_{p-p})/d(\ln V) \approx 17.0$ or $d(\ln W_{p-p})/dP = -0.44 \text{ GPa}^{-1}$; using instead $\gamma = 1.62$ (Ref. 63) gives a value of -0.52 GPa^{-1} .

In order to compare this value with the experimental data, we assume that the various components of $W_e(P)$ can be calculated from the corresponding parts of $\rho(P)$. dW_{p-e}/dP can be found by differentiating Eq. (12) with respect to volume and using the expression (14b) for γ . Assuming the pressure dependence of Λ to be equal to that of Λ_{tr} (Ref. 53) given above, and inserting the known

pressure dependence of $N(E_F)$ (Ref. 49) we find $d(\ln W_{p-e})/dP \approx -8 \times 10^{-2} \text{ GPa}^{-1}$ at $T > \Theta$, which is small compared to the estimated pressure dependence of W_{p-p} . We can then use the data for $d(\ln \lambda)/dP$ above T_C to find experimental values of W_{p-p} in models I and II presented above. The results are $d(\ln W_{p-p})/dP = -0.45 \text{ GPa}^{-1}$ and -0.57 GPa^{-1} , respectively, at 400 K, in very good agreement with the theoretical values. This is somewhat surprising, since the model used is very crude; as shown by Pettersson⁶⁵ it is necessary to use a much more detailed model to obtain good agreement between theory and experiment for the alkali halides.

Finally, we have used the experimental data for the pressure dependence of W_{p-p} and W_e , together with the estimated pressure dependence of W_{p-e} , to calculate $d(\ln \lambda)/dP$ at $T < T_C$ in the two models. The results are shown in Fig. 10, together with the corresponding experimental data. In these calculations we have made the same assumption regarding the T and P dependence of λ_m as we did for ρ_m , i.e., that $\lambda_m = Ef(T/T_C)$, where f is independent of pressure; furthermore, we have assumed E to be independent of P . It is clear from the figure that model II gives a much better agreement with experiments. We note, however, that if we assume that λ_m completely disappears up to 1 GPa in model I, this model also agrees fairly well with the data. We also note that this is not realistic, since analyzing the data obtained at 1 GPa in the same way as the zero-pressure data always yields a residual magnon term. This analysis thus confirms that model II is a better quantitative model.

We can thus conclude the following about the magnon-thermal-conductivity term λ_m : The magnitude is probably fairly close to that given by model II, i.e., $\lambda_m \approx 1.5 \text{ W m}^{-1} \text{ K}^{-1}$ at 200 K, rising to $2.4 \text{ W m}^{-1} \text{ K}^{-1}$ at 100 K. The uncertainty in these figures is probably high, especially below 150 K, but it is difficult to estimate the numerical errors in the assumptions made. In our model λ_m drops to zero at 45 K, but in reality we expect a more gradual decrease towards zero, since theory⁵⁷ predicts $\lambda_m \propto T^2$ at low temperatures. Our results do not exclude such a dependence since we have omitted phonon-impurity scattering. At high temperatures, the results of model I are in excellent agreement with $\lambda_m \propto T^{-1}$, with a more rapid drop near T_C . In the more realistic model II, however, no simple power law (T^{-n}) seems to be valid for λ_m . Although magnon-magnon scattering is believed to dominate λ_m at high temperatures,⁵⁸ both phonons and electrons also scatter magnons, and our data are not sufficiently accurate to enable us to study these mechanisms in any detail. The pressure dependence of λ_m is probably fairly small, but we cannot deduce an exact value. The results shown in Fig. 10 indicate $d(\ln \lambda_m)/dP = (0 \pm 0.1) \text{ GPa}^{-1}$. We also note that a better agreement with experiment would be obtained in

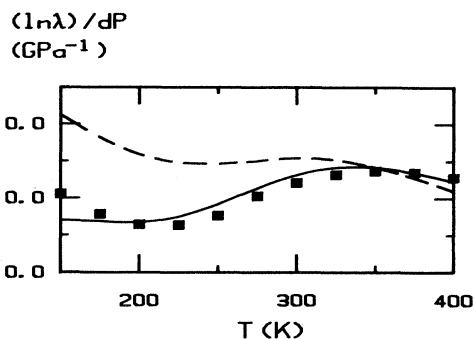


FIG. 10. Pressure dependence of λ as a function of T . Squares denote experimental data, dashed curve model I, and solid curve model II.

the same figure if λ_m was larger near T_C and smaller near 150 K.

V. SUMMARY AND CONCLUSIONS

We give above new, accurate experimental data for the thermal diffusivity and the thermal conductivity of gadolinium as functions of both temperature and pressure. These data differ from most older sets of data in that they can be analyzed in a simple and consistent way, with λ_e , λ_p , and the Lorenz function being smooth functions of temperature. Furthermore, all of these also behave in a normal way as functions of temperature and have magnitudes that are in good agreement with simple theoretical estimates.

The pressure dependence of the lattice thermal conductivity is much larger than the commonly used theoretical approximations indicate. We note that for other metals and alloys we have also found that $d\lambda/dP$ is larger than predicted by the same theory.^{15,16,20} Although hcp Gd might be a special case, it is possible that the standard approximation is not good enough, and that better agreement with theory might be obtained for all metals if a better model were used.

Independently of the model used in analyzing the data we always find a small residual term in λ below T_C that we identify with a magnon heat transport term λ_m . Although the numerical value of this term remains uncertain, our best estimate is that it amounts to about 20% of λ below 200 K. We suggest that the low-temperature thermal conductivity of Gd should be studied further in a strong magnetic field in order to clarify this question further and possibly find a better estimate of the magnitude of λ_m . We also suggest that a theoretical calculation of magnon heat conduction at high temperatures, and near a Curie or Néel transition, including all possible scattering mechanisms, would be of great interest.

¹*Magnetic Properties of Rare Earth Metals*, edited by R. J. Elliot (Plenum, London, 1972).

²*Handbook of the Physics and Chemistry of Rare Earths*, edited by K. A. Gschneidner, Jr. and L. R. Eyring (North-Holland,

Amsterdam, 1978), Vol. 1.

³A. G. A. M. Saleh and N. H. Saunders, *J. Magn. Magn. Mater.* **29**, 197 (1982).

⁴J. B. Sousa *et al.*, *J. Phys. (Paris)* **41**, 573 (1980).

- ⁵S. Arajs and R. V. Colvin, *J. Appl. Phys.* **35**, 1043 (1964).
- ⁶R. W. Powell and B. W. Jolliffe, *Phys. Lett.* **14**, 171 (1965).
- ⁷S. Legvold and F. H. Spedding, U.S. Atomic Energy Commission Report No. ISC-508, 1954 (unpublished).
- ⁸L. Binkele, *High Temp.—High Pressures* **21**, 131 (1989).
- ⁹D. G. S. Chuah and R. Ratnalingam, *J. Low. Temp. Phys.* **14**, 257 (1974).
- ¹⁰W. J. Nellis and S. Legvold, *Phys. Rev.* **180**, 581 (1969).
- ¹¹J. E. Cranch, in *Thermal Conductivity 16*, edited by E. C. Larsen (Plenum, New York, 1983), p. 295.
- ¹²I. I. Novikov, L. P. Filippov, and V. I. Kostyukov, *At. Energ.* **43**, 300 (1977) [*Sov. At. En.* **43**, 943 (1977)].
- ¹³N. G. Aliev and N. V. Volkenshtein, *Zh. Eksp. Teor. Fiz.* **49**, 24 (1965) [*Sov. Phys.—JETP* **22**, 17 (1966)].
- ¹⁴B. Sundqvist, *Phys. Rev. B* **38**, 12 283 (1988).
- ¹⁵B. Sundqvist, in *Proceedings of the 9th International AIRAPT Conference*, edited by C. G. Homan, R. K. MacCrone, and E. Whalley (Elsevier, New York, 1984), Vol. I, pp. 261–268; R. G. Ross, P. Andersson, B. Sundqvist, and G. Bäckström, *Rep. Prog. Phys.* **47**, 1347 (1984).
- ¹⁶P. Jacobsson and B. Sundqvist, *J. Phys. Chem. Solids* **49**, 441 (1988).
- ¹⁷B. Sundqvist and G. Bäckström, *Rev. Sci. Instrum.* **47**, 177 (1976).
- ¹⁸T. E. Scott, in *Handbook of the Physics and Chemistry of Rare Earths*, Ref. 2, p. 606.
- ¹⁹A. J. Ångström, *Ann. Phys. Chem.* **114**, 513 (1861).
- ²⁰P. Jacobsson and B. Sundqvist, *Int. J. Thermophys.* **9**, 577 (1988).
- ²¹O. Sandberg and B. Sundqvist, *J. Appl. Phys.* **53**, 8751 (1982).
- ²²G. Andersson, B. Sundqvist, and G. Bäckström, *J. Appl. Phys.* **65**, 3943 (1989).
- ²³R. R. Birss and S. K. Dey, *Proc. R. Soc. London, Ser. A* **263**, 473 (1961).
- ²⁴J. B. Sousa *et al.*, *J. Phys. F* **9**, L77 (1979); J. B. Sousa *et al.*, *J. Magn. Magn. Mater.* **15–18**, 892 (1980).
- ²⁵Y. S. Touloukian, R. K. Kirby, R. E. Taylor, and P. D. Desai, *Thermophysical Properties of Matter: Vol. 12, Thermal Expansion* (IFI/Plenum, New York, 1977), p. 107.
- ²⁶D. Bloch and A. S. Pavlovic, in *Advances in High Pressure Research*, edited by R. S. Bradley (Academic, London, 1969), Vol. 3, p. 85.
- ²⁷P. Hargraves, R. A. Dunlap, D. J. W. Geldart, and S. P. Ritcey, *Phys. Rev. B* **38**, 2862 (1988).
- ²⁸H. Bartholin and D. Bloch, *J. Phys. Chem. Solids* **29**, 1063 (1968).
- ²⁹W. C. Thoburn, S. Legvold, and F. H. Spedding, *Phys. Rev.* **110**, 1298 (1958).
- ³⁰M. B. Salaman and D. S. Simons, *Phys. Rev. B* **7**, 229 (1973).
- ³¹J. J. Rhyne, in *Magnetic Properties of Rare Earth Metals*, Ref. 1, pp. 162 and 163.
- ³²L. R. Sill and S. Legvold, *Phys. Rev.* **137**, A1139 (1965).
- ³³M. Griffel, R. E. Skochdopole, and F. H. Spedding, *Phys. Rev.* **93**, 657 (1954).
- ³⁴Å. Fransson (unpublished).
- ³⁵M. J. Laubitz, in *Thermal Conductivity*, edited by R. P. Tye, (Academic, London, 1969), Vol. 1 p. 111.
- ³⁶N. Iwata, T. Okamoto, and E. Tatsumoto, *J. Phys. Soc. Jpn.* **24**, 948 (1968).
- ³⁷A. Jayaraman and R. C. Sherwood, *Phys. Rev. Lett.* **12**, 22 (1964).
- ³⁸D. B. McWhan and A. L. Stevens, *Phys. Rev.* **139**, A682 (1965).
- ³⁹A. Nakaue, *J. Less-Common Met.* **60**, 47 (1978).
- ⁴⁰P. W. Bridgman, *Proc. Am. Acad. Arts Sci.* **82**, 97 (1953).
- ⁴¹H. Fujii, H. Tani, T. Okamoto, and E. Tatsumoto, *J. Phys. Soc. Jpn.* **33**, 855 (1972).
- ⁴²H. D. Stromberg and D. R. Stephens, *J. Phys. Chem. Solids* **25**, 1015 (1964).
- ⁴³I. G. Austin and P. K. Mishra, *Philos. Mag.* **15**, 529 (1967).
- ⁴⁴G. Jura and W. A. Stark, Jr., *Rev. Sci. Instrum.* **40**, 656 (1969).
- ⁴⁵H. Bartholin *et al.*, *J. Appl. Phys.* **42**, 1679 (1971).
- ⁴⁶K. P. Rodionov, *Zh. Tekh. Fiz.* **36**, 1287 (1966) [*Sov. Phys.—Tech. Phys.* **11**, 955 (1967)].
- ⁴⁷T.-W.E. Tsang, K. A. Gschneidner, Jr., F. A. Schmidt, and D. K. Thome, *Phys. Rev. B* **31**, 235 (1985).
- ⁴⁸G. Grimvall, *Thermophysical Properties of Materials*, Vol. 18 of *Selected Topics in Solid State Physics*, edited by E. P. Wohlfarth (North-Holland, Amsterdam, 1986).
- ⁴⁹M. I. Darby and N. Richardson, in *Magnetism and Magnetic Materials—1974 (San Francisco)*, Proceedings of the 20th Annual Conference on Magnetism and Magnetic Materials, AIP Conf. Proc. No. 24, edited by C. D. Graham, G. H. Lander, and J. J. Rhyne (AIP, New York, 1975).
- ⁵⁰S. Legvold, in *Magnetic Properties of Rare Earth Metals*, Ref. 1, pp. 335–347.
- ⁵¹N. V. Volkenshtein, V. P. Dyakina, and V. E. Startsev, *Phys. Status Solidi B* **57**, 9 (1973).
- ⁵²A. Jayaraman, in *Handbook of the Physics and Chemistry of Rare Earths*, Ref. 2, pp. 732–735.
- ⁵³B. Sundqvist, J. Neve, and Ö. Rapp, *Phys. Rev. B* **32**, 2200 (1985).
- ⁵⁴A. J. Freeman, in *Handbook of the Physics and Chemistry of Rare Earths*, Ref. 1, pp. 245–260.
- ⁵⁵P. G. De Gennes and J. Friedel, *J. Phys. Chem. Solids* **4**, 71 (1958).
- ⁵⁶M. J. Laubitz, *High Temp.—High Pressures* **4**, 379 (1972).
- ⁵⁷W. B. Yelon and L. Berger, *Phys. Rev. Lett.* **25**, 1207 (1970); D. Valton, J. E. Rives, and Q. Khalid, *Phys. Rev. B* **8**, 1210 (1973); Y. Hsu and L. Berger, *ibid.* **14**, 4059 (1976); A. Kumar, *ibid.* **25**, 3369 (1982).
- ⁵⁸A. R. Mackintosh and H. Bjerrum Møller, in *Magnetic Properties of Rare Earth Metals*, Ref. 1, pp. 228–237.
- ⁵⁹W. H. Butler and R. K. Williams, *Phys. Rev. B* **18**, 6483 (1978).
- ⁶⁰R. Ratnalingam and J. B. Sousa, *J. Low Temp. Phys.* **4**, 401 (1971).
- ⁶¹J. M. Ziman, *Electrons and Phonons* (Oxford University Press, Oxford, 1960), p. 385.
- ⁶²G. K. White, in *Thermal Conductivity: Proceedings of the 8th Conference*, edited by C. Y. Ho and R. E. Taylor (Plenum, New York, 1969), pp. 37–43.
- ⁶³K. A. Gschneidner, Jr., in *Solid State Physics*, edited by F. Seitz and D. Turnbull (Academic, New York, 1964), Vol. 16, pp. 368–418.
- ⁶⁴S. N. Vaidya and G. C. Kennedy, *J. Phys. Chem. Solids* **31**, 2329 (1970).
- ⁶⁵S. Pettersson, *J. Phys. Condensed Matter* **1**, 347 (1989), and references therein.